Multiconnection of Identical Zinc Finger: Implication for DNA Binding Affinity and Unit Modulation of the Three Zinc Finger Domain†

Makoto Nagaoka, Tamaki Kaji, Miki Imanishi, Yuichiro Hori, Wataru Nomura, and Yukio Sugiura*

Institute for Chemical Research, Kyoto University, Uji, Kyoto 611-0011, Japan

Received July 27, 2000; Revised Manuscript Received December 21, 2000

ABSTRACT: Cys_2-His_2-type zinc finger proteins have a tandemly repeated array structure consisting of independent finger modules. They are expected to elevate the DNA binding affinity and specificity by increasing the number of finger modules. To investigate the relation between the number and the DNA binding affinity of the zinc finger, we have designed the two- to four-finger peptides by connecting the central zinc finger (finger 2) of Sp1 with the canonical linker sequence, Thr-Gly-Glu-Lys-Pro. Gel mobility shift assays reveal that the cognate three- and four-finger peptides, Sp1(zf222) and Sp1(zf2222), strongly bind to the predicted target sequences, but the two-finger peptide, Sp1(zf22), does not. Of special interest is the fact that the dissociation constant for Sp1(zf2222) binding to the target DNA is comparable to that for Sp1(zf222). The methylation interference, DNase I and hydroxyl radical footprintings, and circular permutation analyses demonstrate that Sp1(zf2222) binds to its target site with three successive zinc fingers and the binding of the fourth zinc finger is inhibited by DNA bending induced by the binding of the three-finger domain. The present results strongly indicate that the zinc finger protein binds to DNA by the three-finger domain as one binding unit. In addition, this information provides the basis for the design of a novel multifinger protein with high affinity and specificity for long DNA sequences, such as chromosomal DNAs.

A zinc finger motif of the Cys_2-His_2 type is one of the most ubiquitous DNA binding motifs found in eukaryotes and has a tandemly repeated structure consisting of independent modules with the consensus sequence (Tyr, Phe)-X-Cys-$X_{2,4}$-Cys-X_3-Phe-X_5-Leu-X_2-His-X_{3-5}-His-X_{2-6}. Each finger domain is mostly connected by the well-conserved linker (*Krüppel-type* linker, Thr-Gly-Glu-Lys-Pro) and holds as a compact globular $\beta\beta\alpha$ structure by zinc binding with invariant cysteines and histidines. This zinc finger structure also provides the following characteristic DNA binding modes: (1) monomeric and asymmetric DNA binding, (2) independent DNA binding of each zinc finger, and (3) specific base recognition by the amino acid residues at key positions in each finger domain (*1, 2*). To define a protein−DNA interaction mode, several groups have constructed the library of zinc fingers with various DNA binding specificities using the mutagenic or the phage display strategies (*3*−*6*). On the other hand, multifinger proteins based on the tandem array structure of the zinc finger have been created by the connection of two or three units of the naturally occurring three zinc finger protein with a *Krüppel-type* or designed linker (*7*−*9*), and these artificial proteins exhibited a higher affinity than the wild-type for a predicted binding sequence. Therefore, it is of special interest whether the stepwise increase in the number of zinc fingers systematically raises the binding affinity for the target site of DNA.

In this study, novel peptides with two to four central zinc fingers of transcription factor Sp1 connected by the *Krüppel-type* linker were designed, and the increase in their DNA binding affinities was examined. The gel mobility shift assays revealed that the dissociation constants for target DNA are comparable in the cognate three- and four-finger peptides. Methylation interference and DNase I footprinting analyses also clarified that the three- and four-finger peptides bind to DNA with three successive zinc fingers and that the finger at the N-terminal end of the four-finger peptide cannot effectively bind to DNA because of DNA bending at the binding site.

MATERIALS AND METHODS

Chemicals. T4 polynucleotide kinase and restriction enzymes were purchased from New England Biolabs, except for *Age*I obtained from Nippon Gene (Tokyo, Japan). Synthesized oligonucleotides for construction of the genes and substrate DNAs were acquired from Amersham Pharmacia Biotech. Labeled compound [γ-^{32}P]ATP was supplied by DuPont. The plasmid pBS-Sp1-fl was kindly provided by Dr. R. Tjian. All other chemicals were of commercial reagent grade.

Construction of Genes and Peptide Expression. Sp1(zf22), Sp1(zf222), and Sp1(zf2222) were constructed by the connection of two, three, and four central zinc fingers (finger 2) derived from the zinc finger domain of Sp1 with the *Krüppel-type* linker. pEVSp1(zf23), which codes the finger 1-deleted mutant Sp1(zf23), was constructed as previously described (*10*). The new *Age*I site was created at the linker region between fingers 2 and 3 on pEVSp1(zf23). This

† This study was supported in part by a Grant-in-Aid for COE Project "Element Science" (12CE2005), Priority Project "Biometals" (08249103), and Scientific Research (10470493·12470505) from the Ministry of Education, Science, Sports, and Culture, Japan.

* To whom correspondence should be addressed. Phone: +81-774-38-3210. Fax: +81-774-32-3038. E-mail: sugiura@scl.kyoto-u.ac.jp.

10.1021/bi001762+ CCC: $20.00
Published on Web 02/10/2001

construct was renamed as pEVSp1(zf23)′. The finger 2 gene fragments were amplified by PCR with the primer set of pEVSp1(zf23)′ as a template. The amplified fragments which were designed to be flanked by *Xma*I and *Age*I sites at the 5′- and 3′-ends, respectively, were digested with the enzymes and ligated into pEVSp1(zf23)′ at the *Age*I site. The *Age*I enzyme site in the linker region encodes amino acids Thr-Gly, part of the *Krüppel-type* linker peptide. Repeating the step 1−3 times, we created the plasmids pEVSp1(zf22), pEVSp1(zf222), and pEVSp1(zf2222), which code Sp1-(zf22), Sp1(zf222), and Sp1(zf2222), respectively. All sequences were confirmed by an ABI PRISM 377 DNA sequencer. These zinc finger peptides were overexpressed in *Escherichia coli* strain BL21(DE3)pLysS and purified according to the previous paper (*7*).

Preparations of Substrate DNA Fragments. The substrate oligonucleotides contain the target binding site predicted from the binding mode of transcription factor Sp1: 2GCG; 5′-GCG GCG-3′, 3GCG; 5′-GCG GCG GCG-3′, and 4GCG; 5′-GCG GCG GCG GCG-3′. The synthesized oligonucleotides were annealed and inserted in pBluescript II SK+ (Stratagene, CA). The *Hin*dIII−*Xba*I, *Bss*HII−*Sac*I, or *Bss*HII−*Kpn*I fragment was cut out and labeled at the 5′-end by ^{32}P for the experiments.

Circular Dichroism (CD) Measurements. The CD spectra of Sp1(zf22), Sp1(zf222), and Sp1(zf2222) were recorded on a Jasco J-720 spectropolarimeter in 10 mM Tris-HCl (pH 8.0), 50 mM NaCl, 1 mM dithiothreitol, and 3−10 μM zinc finger peptide at 20 °C.

Gel Mobility Shift Assays. Gel mobility shift assays were carried out under the following conditions. Each reaction mixture contained 10 mM Tris-HCl (pH 8.0), 50 mM NaCl, 1 mM dithiothreitol, 0.1 mM $ZnCl_2$, 25 ng/μL poly(dI-dC), 0.05% Nonidet P-40, 5% glycerol, the ^{32}P-end-labeled *Hin*dIII−*Xba*I substrate DNA fragment (∼50 pM), and 150−450 nM zinc finger peptide. After incubation at 20 °C for 30 min, the sample was run on a 12% polyacrylamide gel with Tris−borate buffer at 20 °C. The bands were visualized by autoradiography and quantified with NIH image software (version 1.62). The dissociation constants (K_d) of the Sp1 peptide−DNA fragment complexes were estimated according to the previously reported procedure (*10*).

Methylation Interference Analyses. Methylation interference assays were investigated as previously described (*11*). The binding reaction mixture contained 10 mM Tris-HCl (pH 8.0), 50 mM NaCl, 1 mM dithiothreitol, 0.1 mM $ZnCl_2$, 25 ng/μL poly(dI-dC), 0.05% Nonidet P-40, 5% glycerol, the ^{32}P-end-labeled *Hin*dIII−*Xba*I-methylated DNA fragment (approximately 500 Kcpm), and 20−50 nM zinc finger peptides. To examine both the strong and weak base contacts in the methylation interference experiment, we selected the experimental conditions such that the peptide/DNA molar ratio in the binding reaction was about 10−20% bound.

DNase I Footprinting Analyses. DNase I footprinting experiments were performed according to the method of Brenowitz et al. (*12*). The binding reaction mixture contained 20 mM Tris-HCl (pH 8.0), 5 mM $CaCl_2$, 10 mM $MgCl_2$, 20 ng/μL sonicated calf thymus DNA, the 5′-end-labeled *Bss*HII−*Sac*I or *Bss*HII−*Kpn*I substrate DNA fragment (approximately 15 000 cpm), and 0−3.5 μM peptide. After incubation at 20 °C for 30 min, the sample was digested with DNase I (0.7 milliunit/μL) at 20 °C for 2 min. The reaction was stopped by the addition of 20 μL of DNase I stop solution (0.1 M EDTA and 0.6 M sodium acetate) and 40 μL of phenol/chloroform. After ethanol precipitation, the cleavage products were analyzed on a 10% polyacrylamide/7 M urea sequencing gel. The bands were visualized by autoradiography and analyzed by Storm 820 (Amersham Pharmacia Biotech).

Hydroxyl Radical Footprinting Analyses. Hydroxyl radical footprinting experiments were carried out according to the method reported by Tullius et al. (*13*). The binding reaction mixture contained 20 ng/μL sonicated calf thymus DNA, the 5′-end-labeled *Bss*HII−*Sac*I or *Bss*HII−*Kpn*I substrate DNA fragment (approximately 15 000 cpm), and 0−3.5 μM peptide. After incubation at 20 °C for 30 min, the sample was cleaved by the addition of 100 μM ferrous ammonium sulfate, 200 μM EDTA, and 0.003% hydrogen peroxide at 20 °C for 1 min. The reaction was quenched by adding 20 μL of hydroxyl radical stop solution (0.135 M thiourea, 0.135 M EDTA, and 0.6 M sodium acetate). After phenol extraction and ethanol precipitation, the cleavage products were analyzed on a 10% polyacrylamide/7 M urea sequencing gel. The bands were visualized by autoradiography and quantified with ImageQuant software (version 5.1).

Circular Permutation Assays. Two plasmid DNAs for the creation of circularly permuted fragments were designed by linking two units of the multicloning site of pUC19 with a target DNA site, 3GCG or 4GCG. The digestion of the plasmids by *Sal*I, *Xba*I, *Bam*HI, *Sma*I, or *Kpn*I leads to the preparation of five kinds of circularly permuted substrates for each target site. The binding reaction mixture contained 89 mM Tris−borate, 5% glycerol, 0.4 μg of circularly permuted substrate DNA, 3 μM peptide, and 9.0 μg of vector fragment. No special treatments were performed to remove vector fragment which serves as competitor DNA. After incubation at 20 °C for 30 min, the sample was run on a 5% polyacrylamide gel with Tris−borate buffer at 20 °C. The bands were visualized by ethidium fluorescence and analyzed by ImageMaster 1D Elite software (version 3.0).

RESULTS

Design of Multiple Finger Peptides with Identical Zinc Fingers Connected by a Krüppel-Type Linker. Zinc finger proteins of the Cys_2-His_2 type have a modular structure, and each finger module recognizes 3−4 bases of DNA. The appropriate regulation of the number of zinc fingers probably leads to the creation of zinc fingers with a higher affinity for the longer recognition sites. However, direct and/or indirect interactions between the zinc fingers are not negligible, because they often have significant effects on the DNA binding by the zinc fingers (*14*). To evaluate the increase in the DNA binding affinity versus the number of zinc fingers, the multiplication of identical zinc fingers is essential.

Sp1(530−623), which contains the three zinc finger domain of Sp1, strongly binds to the GC box (5′-GGG-GCG-GGGCC-3′), and each zinc finger recognizes the 3 or 5 bp subsite in an antiparallel fashion (Figure 1A; *10*, *11*). The middle zinc finger (finger 2) predominantly recognizes the middle triplet, 5′-GCG-3′, as shown in the cases of fingers 1 and 3 of Zif268 based on crystallographic evidence (*1*, *2*, *10*, *11*, *15*, *16*). Namely, Arg(−1) and Arg(6) are involved

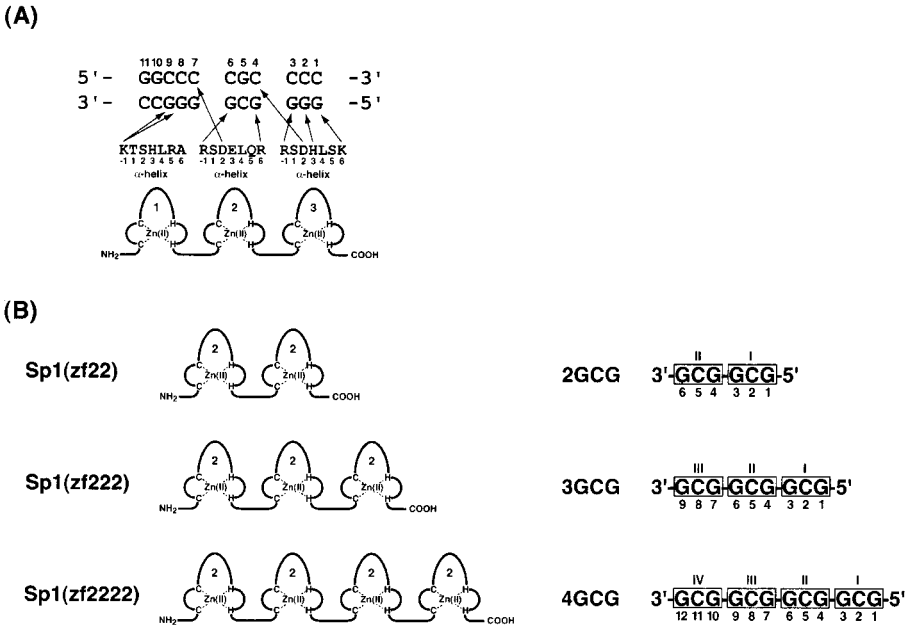

FIGURE 1: (A) Three zinc finger domain of Sp1 and its binding sequence. (B) Artificial zinc finger peptides with identical zinc finger arrays, Sp1(zf22), Sp1(zf222), and Sp1(zf2222), and their predicted binding sequences. The sequences of the guanine-rich strand are only shown with numbering in the direction from the 5′- to the 3′-end. Roman numerals represent the number of a subsite consisting of a 5′-GCG-3′ triplet.

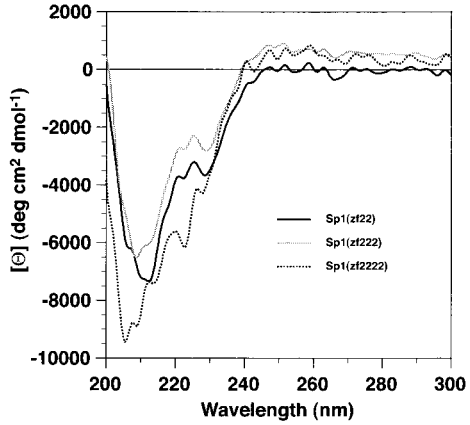

FIGURE 2: CD spectra of Sp1(zf22), Sp1(zf222), and Sp1(zf2222) in the presence of Zn(II) at 20 °C. The concentrations of the zinc finger peptides were 10 μM Sp1(zf22), 10 μM Sp1(zf222), and 3 μM Sp1(zf2222).

in the direct recognition of the guanine bases at the 5′- and 3′-ends in the 5′-GCG-3′ subsite, respectively (the numbers in parentheses show the relative position to the start site of an α-helix). By linking two to four Sp1 zinc finger 2s with the *Krüppel-type* linker, cognate three zinc finger peptides, Sp1(zf22), Sp1(zf222), and Sp1(zf2222), were created (Figure 1B). The predicted target DNA sequences for these peptides contain the same number of 5′-GCG-3′ subsites (Figure 1B).

In the absence of Zn(II) binding, the CD spectrum of these peptides demonstrated no Cotton effects in the far-UV region that show random coil structure. Their CD features in the presence of Zn(II) complexation clearly gave negative Cotton effects, indicating that these peptides form an ordered secondary structure with a helical conformation by Zn(II) binding (Figure 2).

Evaluation of DNA Binding Affinity of Sp1(zf22), Sp1-(zf222), and Sp1(zf2222). By gel mobility shift assays (Figure 3), we obtained the dissociation constants (K_d) of these peptide−*n*GCG (n = 2−4) complexes as summarized in Table 1. The DNA binding activities did not change in the presence of 10−100 μM Zn(II). Panels A and C in Figure 3 show the results of Sp1(zf22) in the complex with 2GCG and 4GCG, respectively. Only in lane 11 of both experiments were smeared bands detected at the high concentration of peptides. In contrast, the light and clear mobility-shifted bands were visualized in the Sp1(zf22)−3GCG complex (Figure 3B, lanes 8−10), but the ratio of the peptide-bound band did not increase according to the peptide concentration. These results indicate that Sp1(zf22) forms no stable complexes with *n*GCG (n = 2−4). The dissociation constants for the complex of Sp1(zf22)−*n*GCG (n = 2−4) were not precisely determined.

Table 1: Dissociation Constants (K_d) for Spl(zf22), Sp1(zf222), and Sp1(zf2222) Binding to 2GCG, 3GCG, and 4GCG

	K_d (nM)[a]		
binding site	Sp1(zf22)	Sp1(zf222)	Sp1(zf2222)
2GCG	ND[b]	>3000	>3000
3GCG	>3000	61.4 ± 10.8	32.4 ± 8.50
4GCG	ND	103 ± 11.6	18.2 ± 2.25

[a] Apparent dissociation constants are determined by titration using a gel mobility shift assay as described under Materials and Methods. Values are averages of two independent determinations with standard errors. [b] ND, not determined.

Panels D−F show the results for Sp1(zf222). Although the peptide-bound bands were observed only at the high peptide concentration in panel D, the ratio of the peptide-bound band gradually increased with peptide concentration in panels E and F. The dissociation constants for Sp1(zf222) binding to 3GCG and 4GCG were 61.4 and 103 nM, respectively. The same binding specificity was detected in the case of Sp1(zf2222) (panels G−I). The K_d values for the Sp1(zf2222)−3GCG and −4GCG complexes were 32.4

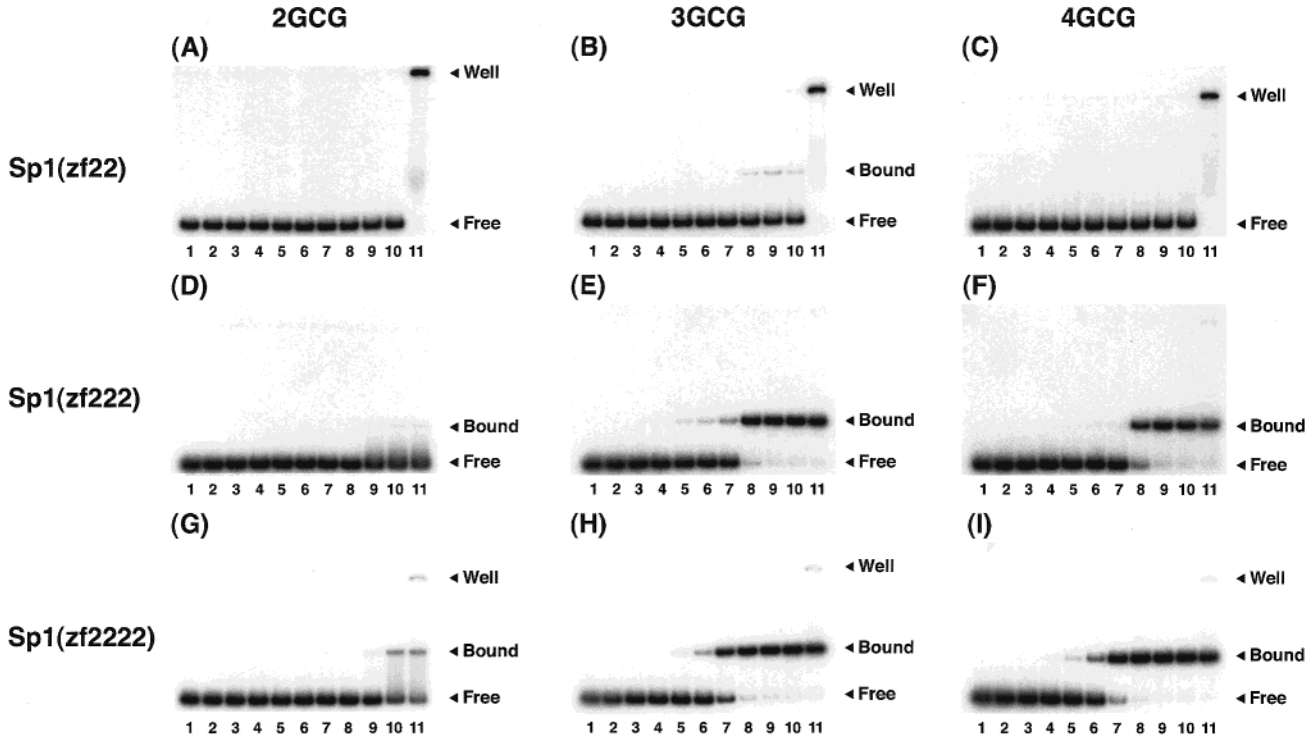

FIGURE 3: Gel mobility shift assays for Sp1(zf22), Sp1(zf222), and Sp1(zf2222). (A−C) Sp1(zf22) binding to 2GCG, 3GCG, and 4GCG, respectively: lanes 1−11 contain 0, 1, 3, 10, 30, 100, 300, 1000, 3000, 10 000, and 30 000 nM peptide, respectively. (D−F) Sp1(zf222) binding to 2GCG, 3GCG, and 4GCG, respectively: lanes 1−11 contain 0, 0.1, 0.3, 1, 3, 10, 30, 100, 300, 1000, and 3000 nM peptide, respectively. (G−I) Sp1(zf2222) binding to 2GCG, 3GCG, and 4GCG, respectively: lanes 1−11 contain 0, 0.1, 0.3, 1, 3, 10, 30, 100, 300, 1000, and 3000 nM peptide, respectively.

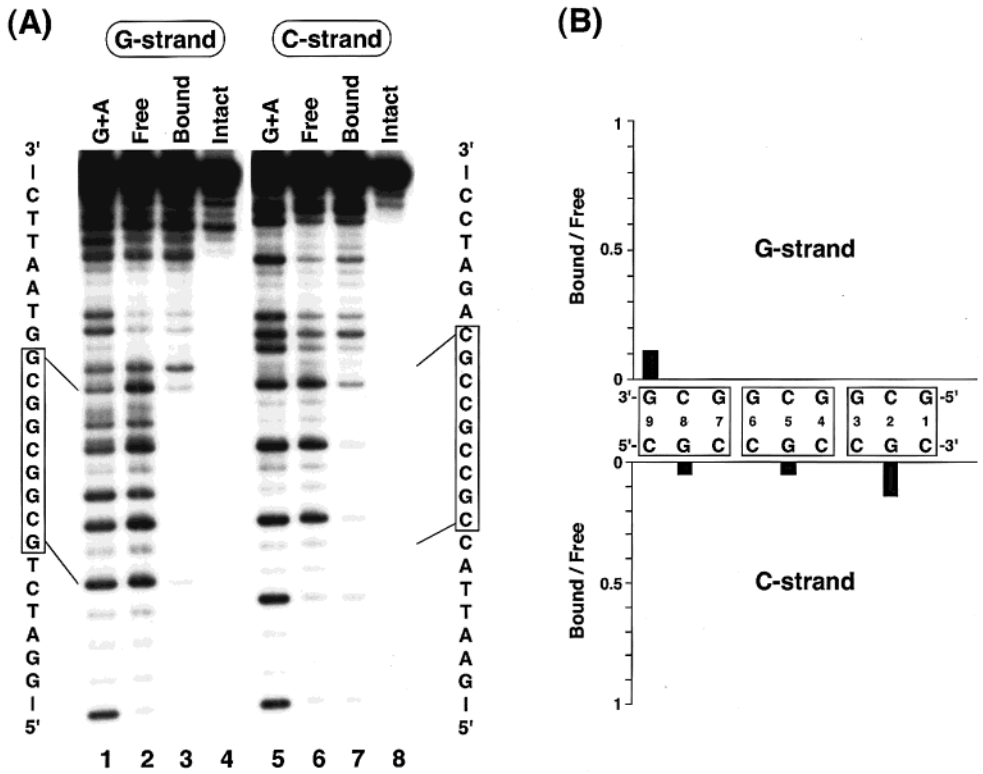

FIGURE 4: (A) Methylation interference analysis for Sp1(zf222) binding to 3GCG. The left (lanes 1−4) and right (lanes 5−8) panels show the results for the G- and C-strands, respectively. Lanes 1 and 5, G + A (Maxam−Gilbert reaction products); lanes 2, 3, 6, and 7, free and peptide-bound DNA samples; lanes 4 and 8, intact DNA. (B) Histogram showing the extent of methylation interference by Sp1(zf222). An autoradiogram of the gel was scanned with a densitometer, and the extent of interference was calculated as the ratio of the cutting probabilities for the two bands (B/F).

and 18.2 nM, respectively. From these results, Sp1(zf222) and Sp1(zf2222) strongly bind to 3GCG and 4GCG, suggesting that the combination of three or more zinc fingers with DNA consisting of three or more 3 bp subsites is

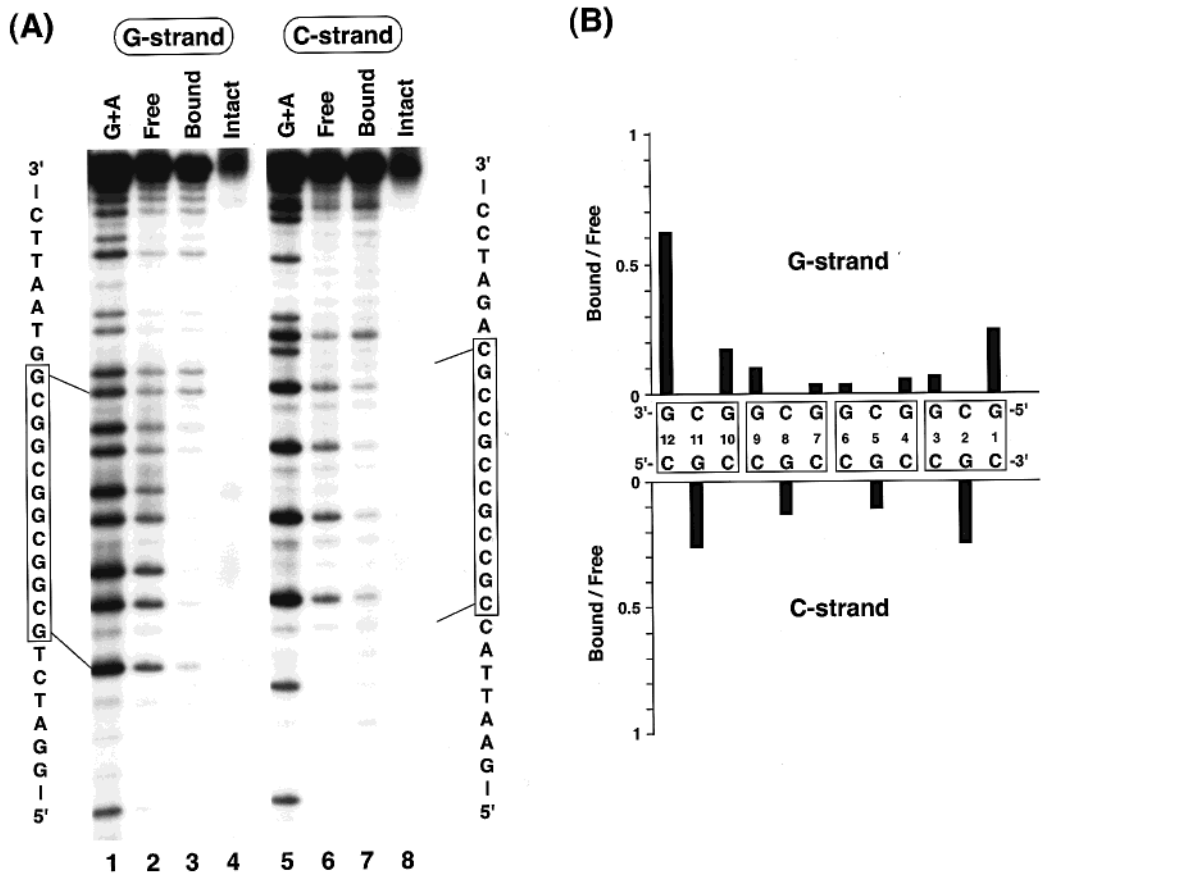

FIGURE 5: (A) Methylation interference analysis for Sp1(zf2222) binding to 4GCG. The left (lanes 1−4) and right (lanes 5−8) panels show the results for the G- and C-strands, respectively. Lanes 1 and 5, G + A (Maxam−Gilbert reaction products); lanes 2, 3, 6, and 7, free and peptide-bound DNA samples; lanes 4 and 8, intact DNA. (B) Histogram showing the extent of methylation interference by Sp1(zf2222). An autoradiogram of the gel was scanned with a densitometer, and the extent of the interference was calculated as the ratio of the cutting probabilities for the two bands (B/F).

required for the formation of a stable zinc finger−DNA complex with a nanomolar dissociation constant.

Specific Base Recognition Analysis Using Methylation Interference Assay. Figures 4 and 5 show the results of the methylation interference assays for Sp1(zf222) and Sp1-(zf2222). From the results of the gel mobility shift assays, Sp1(zf222) and Sp1(zf2222) bind to 3GCG and 4GCG with a higher affinity than the other DNAs, respectively. Therefore, we carried out the experiment using such peptide−DNA combinations. In Figure 4, the electrophoretic result (panel A) and the densitometric analysis (panel B) for Sp1(zf222) are shown. The contacts of all of the guanine bases in the binding site were strongly interfered with by the methylation. Namely, the guanine bases at positions 1, 3, 4, 7, and 9 in the guanine-rich strand (G-strand) and at positions 2, 5, and 8 in cytosine-rich strand (C-strand) are evidently recognized by the three zinc fingers of Sp1(zf222). This base recognition pattern at each subsite is consistent with that observed in finger 2 of Sp1. On the other hand, Sp1(zf2222) showed strong contacts with the guanine bases at positions 3, 4, 6, 7, 9, and 10 in the G-strand and at positions 5 and 8 in the C-strand and made weak contacts with the residual guanine bases in the binding site (Figure 5). This evidence indicates that Sp1(zf2222) mainly recognizes the two subsites, II and III.

DNA Binding Mode Analysis by DNase I Footprinting. In the previous analysis of the interaction between the three zinc finger domain of Sp1 and the GC box by DNase I

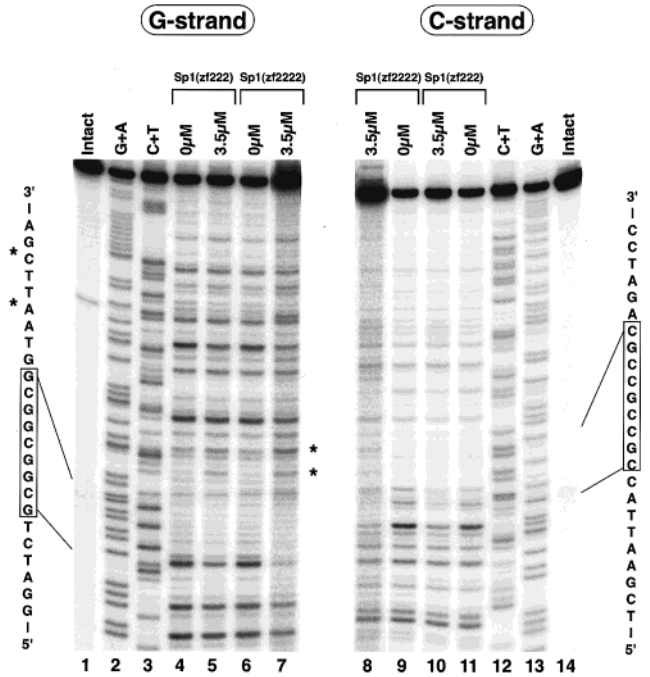

FIGURE 6: DNase I footprinting analyses for Sp1(zf222) and Sp1-(zf2222) binding to 3GCG. The left (lanes 1−7) and right (lanes 8−14) panels show the results for the G- and C-strands, respectively. The asterisks represent enhanced sites of cleavage. Lanes 1 and 14, intact DNA; lanes 2 and 13, G + A (Maxam−Gilbert reaction products); lanes 3 and 12, C + T (Maxam−Gilbert reaction products); lanes 4, 5, 10, and 11, Sp1(zf222); lanes 6−9, Sp1-(zf2222). Peptide concentrations are noted in the figures.

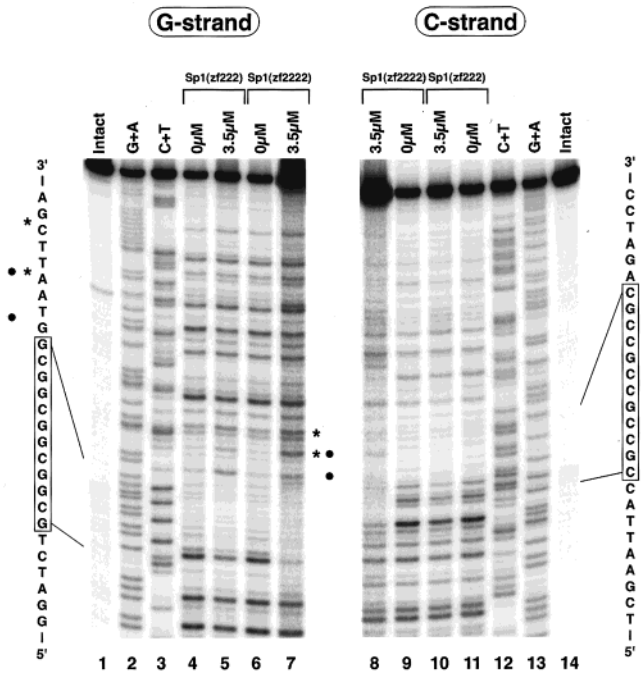

FIGURE 7: DNase I footprinting analyses for Sp1(zf222) and Sp1(zf2222) binding to 4GCG. The left (lanes 1−7) and right (lanes 8−14) panels show the results for the G- and C-strands, respectively. The asterisks and filled circles represent enhanced sites of cleavage. Lanes 1 and 14, intact DNA; lanes 2 and 13, G + A (Maxam−Gilbert reaction products); lanes 3 and 12, C + T (Maxam−Gilbert reaction products); lanes 4, 5, 10, and 11, Sp1(zf222); lanes 6−9, Sp1(zf2222). Peptide concentrations are noted in the figures.

footprinting, the hypersensitive cleavage was detectable at the 3′-portion of the GC box in the G-strand (*17*). The hypersensitivity of the protein-bound DNA in DNase I cleavage is due to the conformational change in DNA induced by the protein binding (*18*, *19*). To examine the binding site and the structural change in DNA induced by the binding of Sp1(zf222) and Sp1(zf2222) to 3GCG and 4GCG, we performed DNase I footprinting analyses. Figure 6 shows the results for 3GCG. In the case of Sp1(zf222), the peptide exactly binds to the predicted binding site, because the protected region is restricted within the site. On the contrary, Sp1(zf2222) inhibited the digestion of DNA by DNase I not only at the 3GCG site but also in the 5−6 bp regions on either side of the binding site, suggesting the presence of several binding modes of Sp1(zf2222) to 3GCG. The hypersensitive cleavages were induced at the 3′-portion outside the binding site in the G-strand by the binding of Sp1(zf222) and Sp1(zf2222). Figure 7 shows the results for 4GCG. In the case of Sp1(zf2222), the same protection pattern as that for 3GCG was acquired. Sp1(zf222) protected all bases in the binding site from the DNase I digestion. For both peptides, hypersensitive cleavages were newly observed at the 5′-GT-3′ step of the 3′-portion of GC box in the G-strand in addition to the same positions as that for 3GCG.

Detection of DNA Conformational Change by Hydroxyl Radical Footprinting and Circular Permutation Analyses. Figure 8 denotes the results of hydroxyl radical footprinting analyses of the G-strands of 3GCG and 4GCG for Sp1(zf222) and Sp1(zf2222). For each peptide−DNA combination, inhibition of cleavage by peptide binding was observed at the binding site. In addition, the cleavage intensities at the 5′-portion outside the binding site in the existence of peptide were stronger than those in no peptide, suggesting that the local conformational change of DNA by peptide binding

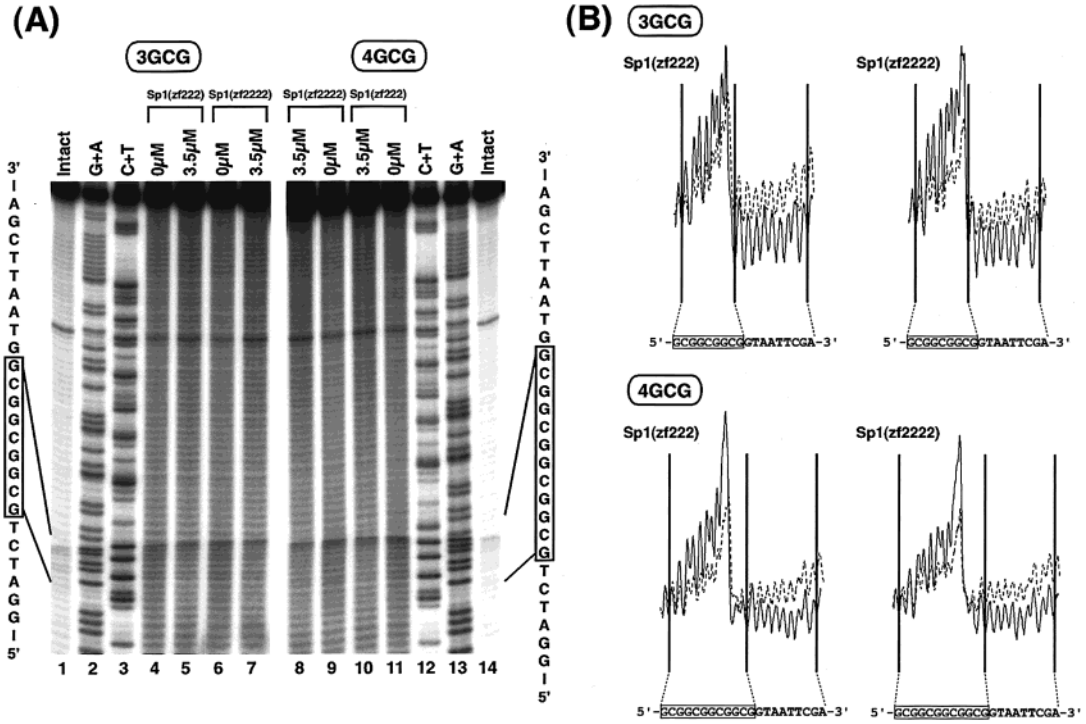

FIGURE 8: Hydroxyl radical footprinting analyses for Sp1(zf222) and Sp1(zf2222) binding to 3GCG and 4GCG. (A) Electrophoretic results of hydroxyl radical footprinting analyses. The left (lanes 1−7) and right (lanes 8−14) panels show the results for the G-strand of 3GCG and 4GCG, respectively. Lanes 1 and 14, intact DNA; lanes 2 and 13, G + A (Maxam−Gilbert reaction products); lanes 3 and 12, C + T (Maxam−Gilbert reaction products); lanes 4, 5, 10, and 11, Sp1(zf222); lanes 6−9, Sp1(zf2222). Peptide concentrations are noted in the figures. (B) Densitometric analyses of the electrophoretic results. Solid and dotted lines denote the cleavage intensities in the absence and presence of the peptide, respectively

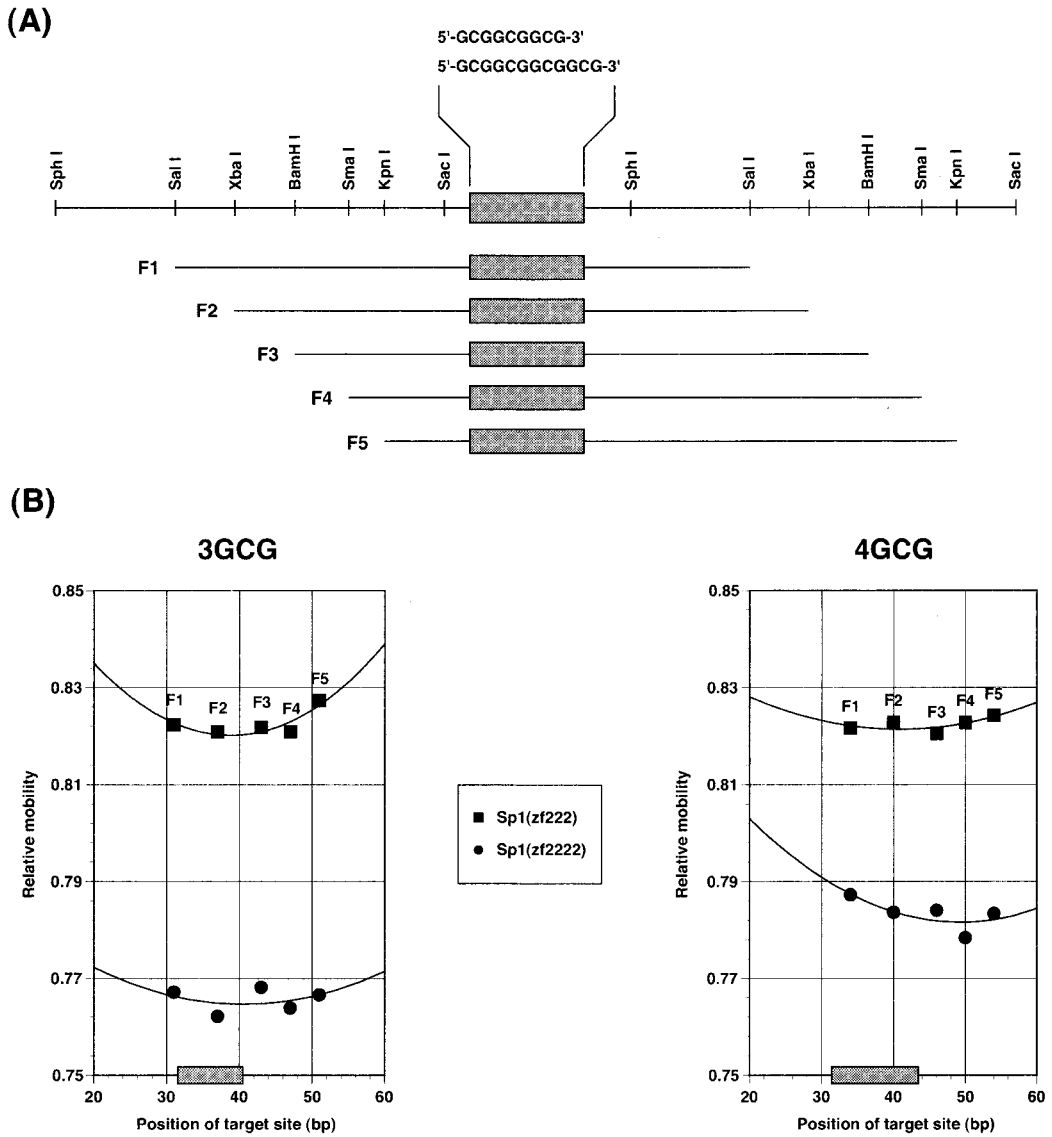

FIGURE 9: Structure of DNA constructs and results of circular permutation assay. (A) Circularly permuted fragments, F1−F5, generated by digestion with five restriction enzymes. The relative position of the target sequence represented by the shaded rectangle is shown for each fragment. (B) Relative mobility curve from the electrophoretic results of circular permutation assay. The relative mobility (μ_{bound}/μ_{free}) of the complex of peptide with each fragment is plotted as a function of the position of the binding site. The curve fitting of the points is based on the calculated best fit of a second-order polynomial function. The position of the binding site is measured from the central cytosine of the second 5′-GCG-3′ triplet to the 3′-end of the fragment. The binding site is shown in each graph as a shaded rectangle.

occurs at the 3′-portion near the binding site in the G-strand.

Moreover, we employed the circular permutation analysis to investigate the conformational change of DNA such as bending induced by peptide binding. The relative mobility of the band of peptide−DNA complex to that of free DNA is summarized as a function of the position of the binding site (Figure 9B). Each peptide showed high relative mobility in the binding to a circularly permuted fragment such as F1 or F5. On the contrary, the relative mobility was low when the peptides bind to F3 and F4 in which the binding site is 5′-shifted from the center in the G-strand. These results indicate that DNA is bent at the 3′-portion near the binding site upon the binding of peptides.

DISCUSSION

Relation between the Number and DNA Binding Affinity of the Zinc Finger. This study demonstrates that the two-finger peptide, Sp1(zf22), does not bind to the predicted binding sequence with high affinity. On the other hand, the two-finger peptide Sp1(zf23) and the other natural two-finger proteins evidently specifically bind to their target sequences (*10*, *20*, *21*). In them, two zinc fingers, in which base recognition modes by amino acid residues at key positions in the α-helix are distinct from each other, are connected. Presumably, the connection of different types of two zinc fingers is essential for the DNA binding of the two-finger peptides. The bindings of the zinc finger proteins induce a conformational change in DNA with an enlarged major groove at the binding site (*2*, *22*). Local helical parameters for the DNA site suggest that the extent of the change at each subsite depends on the types of zinc fingers (*1*, *2*). The variety in the extent may play an important role in the stabilization of the two-finger protein−DNA complex. This evidence indicates that the two zinc finger domain is not

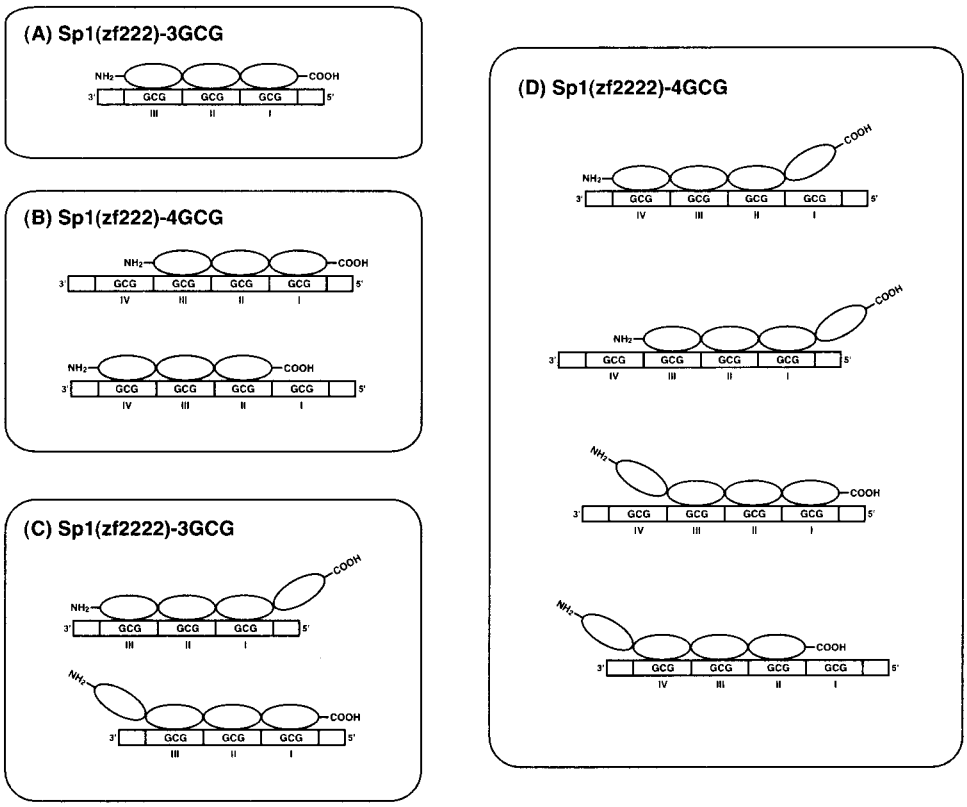

FIGURE 10: Schematic representation of Sp1(zf222) and Sp1(zf2222) binding to 3GCG and 4GCG. (A) Sp1(zf222)−3GCG complex, (B) Sp1(zf222)−4GCG complexes, (C) Sp1(zf2222)−3GCG complexes, and (D) Sp1(zf2222)−4GCG complexes. Ellipsoids and squares denote zinc finger domains and G-strand DNAs, respectively.

always sufficient for effective DNA binding and that its DNA interaction requires a special binding character.

The connection of one or two zinc fingers to Sp1(zf22) induces a high-affinity binding to DNA. The K_d values of Sp1(zf222) and Sp1(zf2222) for 3GCG and 4GCG are 61.4 and 18.2 nM, respectively. The affinity of the latter for the predicted sequence is only 3.4-fold higher than that of the former. In contrast, the relative K_d value of the three-finger peptide Sp1(530−623) normalized to that of the two-finger peptide Sp1(zf23) is 89 (*10*). With respect to the increase in the DNA binding affinity, the addition of one zinc finger to the two-finger peptide is 26-fold higher than that to the three-finger peptide. These results suggest that the fourth zinc finger in Sp1(zf2222) may be ineffective for increasing the DNA binding affinity and that the elevation of the affinity with the increasing number of cognate zinc finger peptides is saturated with the three zinc finger.

DNA Binding Modes of Sp1(zf222) and Sp1(zf2222). Sp1-(zf222) and Sp1(zf2222) form a 1:1 complex with DNA, because their mobility-shifted bands are clearly single in the gel mobility shift assays and the DNA binding mode of the Cys_2-His_2-type zinc finger protein is monomeric (*1*, *2*, *20*). Indeed, Sp1(zf222) and Sp1(zf2222) recognize three or more GCG subsites of 3GCG and 4GCG with three or more successive zinc fingers. From the results of the methylation interference and DNase I footprinting experiments, Sp1-(zf222) binds to three GCG subsites and recognizes all the guanine bases by its three zinc fingers in the Sp1(zf222)−3GCG complex (Figure 10A). This binding pattern suggests the existence of two binding modes for Sp1(zf222) to 4GCG: binding to subsites I−III and II−IV (Figure 10B). The DNase I footprinting pattern for the Sp1(zf222)−4GCG complex, in which *four* GCG subsites are all protected from DNase I cleavage by *three* zinc fingers and an additional pair of hypersensitive cleavages shifted from the original pair by 3 bp is observed, also supports this postulation.

On the contrary, the binding modes of Sp1(zf2222) to 3GCG and 4GCG appear to be more complex. From the results of the methylation interference, the central two GCGs are strongly recognized, and the two GCG subsites at both ends are weakly recognized in the Sp1(zf2222)−4GCG complex. This evidence shows that the zinc finger at the N- *or* C-terminal does not strongly contact the guanine bases. Namely, Sp1(zf2222) utilizes three successive zinc fingers, and the N-terminal or C-terminal zinc finger, like a *free* zinc finger, does not significantly act. The existence of this *free* zinc finger may block the DNase I cleavage outside the binding site by its steric hindrance (Figure 7). On the basis of this model, several types of binding complexes are proposed for the interaction between Sp1(zf2222) and 4GCG (Figure 10D). The results of the DNase I footprinting suggest that the versatility of the DNA binding of Sp1(zf2222) is similarly applicable to its binding to 3GCG (Figures 7 and 10C).

Relation between Conformational Change and DNA Binding Affinity of DNA. The hypersensitivity of DNase I cleavage was observed at the 3′-portion outside the binding site in the G-strand by the binding of Sp1(zf222) or Sp1(zf2222). This type of hypersensitivity has also been detected by the binding of the three-finger peptide [Sp1(530−623)] and not by the binding of the two-finger peptide without finger 1 of Sp1 [Sp1(zf23)] (*10*). The cleavage by the hydroxyl radical at the region was also increased by the binding of peptides. In general, the increase in cleavage of peptide-bound DNA

by DNase I and hydroxyl radicals is due to the sequence bent toward the major groove induced by peptide binding (*18*, *23*). Furthermore, the change in relative mobility of the peptide−DNA complex in circular permutation assays clearly shows that the DNA bending exists and the bend center is situated at the minimum point of relative mobility (*24*). Sjøttem and co-workers reported that the DNA bend of 65° is induced at the 3′-end of the GC box in the G-strand by the binding of the zinc finger domain of native Sp1 (*25*). From our circular permutation assay of Sp1(zf222) or Sp1-(zf2222), the bend center is located at the same region. However, the bend angle is smaller because the difference of the relative mobilities of peptide−DNA complexes is slight between each fragment in our experimental system. Moreover, the extent of hypersensitive cleavage in the footprinting experiments described above was weaker than that in Sp1(530−623) (*10*). Together with this evidence, the results of footprinting and circular permutation assays presented here suggest that moderate DNA bending toward the major groove occurs at the 3′-portion apart from the binding site by several base pairs in the G-strand only by the binding of a three or more zinc finger peptide. The zinc finger protein binds to DNA in an antiparallel fashion; the direction of the peptide chain is antiparallel to that of the DNA chain mainly recognized. Consequently, in the Sp1-(zf2222)−4GCG complex, the DNA bending toward the major groove occurs near the recognition site for the N-terminal zinc finger of Sp1(zf2222). The zinc finger peptide binds to DNA with its α-helix locating on the major groove (*1*, *2*, *20*). If Sp1(zf2222) binds to DNA with three zinc fingers at the C-terminal portion, it cannot utilize the N-terminal zinc finger in DNA binding due to DNA bending toward the major groove. Therefore, the four-finger peptide uses only three successive zinc fingers in DNA binding and has an affinity for DNA close to that of the three-finger peptide.

Perspective to the Design of Multifinger Protein. In this study, we reported that (1) a two zinc finger protein is required for special DNA binding and is always insufficient, (2) the elevation of binding affinity to a target sequence is saturated at the three zinc finger in the zinc finger−DNA interaction, and (3) the saturation in DNA binding affinity is elucidated by the DNA binding modes of the three- and four-finger peptides with the induction of DNA bending. Probably, the design of the multifinger protein with a long recognition sequence is achieved by the increase in the zinc finger number because of its modular structure. Thus far, two designs of multifinger peptides with canonical linker sequences have been accomplished (*7*, *8*). The number of zinc fingers in them is six or nine, namely, multiples of three. Their DNA binding affinities are about 10−100-fold higher than those of the native three-finger proteins. On the other hand, Pabo and his co-worker succeeded in constructing the six-finger protein with a femtomolar dissociation constant for DNA (*9*). Based on the linkage of two units of the three-finger domain which is not with a *Krüppel-type* linker but with a designed longer linker, this design indicates the importance of the linker sequence. Our experiments suggest that the three-finger domain induces DNA bending. Thus, the linker between the third and fourth fingers should be designed to adequately fit the fourth finger into the major groove in the presence of a structural change. The canonical *Krüppel-type* linker is allowed for the linkers between the fourth and fifth or fifth and sixth fingers, because the fourth and fifth fingers, which are independent of the first-to-third-finger domain, act as a one- or two-finger domain without induction of a conformational change in DNA. This concept leads to the rational design of multifinger proteins. It is convenient to define a three-finger domain as one unit and to properly design the linker between the three-finger units. The design of artificial zinc finger proteins with high specificity and affinity can be achieved in this way. The natural multifinger proteins such as transcription factor IIIA bind to DNA without using all of the fingers (*26*−*28*). During the *post-genome* era, the multifinger proteins consisting of several units of three fingers might be discovered. In addition, such multi zinc finger peptides may be promising as a new tool in future gene research.

ACKNOWLEDGMENT

We thank Yumiko Uno for assistance in the preparation of peptides.

REFERENCES

1. Pavletich, N. P., and Pabo, C. O. (1991) *Science 252*, 809−817.
2. Elrod-Erickson, M., Rould, M. A., Nekludova, L., and Pabo, C. O. (1996) *Structure 4*, 1171−1180.
3. Reber, E. J., and Pabo, C. O. (1994) *Science 263*, 671−673.
4. Choo, Y., and Klug, A. (1994) *Proc. Natl. Acad. Sci. U.S.A. 91*, 11163−11167.
5. Choo, Y., and Klug, A. (1994) *Proc. Natl. Acad. Sci. U.S.A. 91*, 11168−11172.
6. Jamieson, A. C., Kim, S.-H., and Wells, J. A. (1994) *Biochemistry 33*, 5689−5695.
7. Kamiuchi, T., Abe, E., Imanishi, M., Kaji, T., Nagaoka, M., and Sugiura, Y. (1998) *Biochemistry 37*, 13827−13834.
8. Liu, Q., Segal, D. J., Ghiara, J. B., and Barbas, C. F., III (1997) *Proc. Natl. Acad. Sci. U.S.A. 94*, 5525−5530.
9. Kim, J.-S., and Pabo, C. O. (1998) *Proc. Natl. Acad. Sci. U.S.A. 95*, 2812−2817.
10. Yokono, M., Saegusa, N., Matsushita, K., and Sugiura, Y. (1998) *Biochemistry 37*, 6824−6832.
11. Kuwahara, J., Yonezawa, A., Futamura, M., and Sugiura, Y. (1993) *Biochemistry 32*, 5994−6001.
12. Brenowitz, M., Senear, D. F., Shea, M. A., and Ackers, G. K. (1986) *Methods Enzymol. 130*, 132−181.
13. Tullius, T. D., Dombroski, B. A., Churchill, M. E. A., and Kam, L. (1987) *Methods Enzymol. 155*, 537−558.
14. Wuttke, D. S., Foster, M. P., Case, D. A., Gottesfeld, J. M., and Wright, P. E. (1997) *J. Mol. Biol. 273*, 183−206.
15. Kriwacki, R. W., Schultz, S. C., Steitz, T. A., and Caradonna, J. P. (1992) *Proc. Natl. Acad. Sci. U.S.A. 89*, 9759−9763.
16. Narayan, V. A., Kriwacki, R. W., and Caradonna, J. P. (1997) *J. Biol. Chem. 272*, 7801−7809.
17. Nagaoka, M., and Sugiura, Y. (1996) *Biochemistry 35*, 8761−8768.
18. Suck, D., Lahm, A., and Oefner, C. (1988) *Nature 332*, 464−468.
19. Travers, A. A. (1989) *Annu. Rev. Biochem. 58*, 427−452.
20. Fairall, L., Schwabe, J. W. R., Chapman, L., Finch, J. T., and Rhodes, D. (1993) *Nature 366*, 483−487.
21. Thukral, S. K., Morrison, M. L., and Young, E. T. (1991) *Proc. Natl. Acad. Sci. U.S.A. 88*, 9188−9192.
22. Nekludova, L., and Pabo, C. O. (1994) *Proc. Natl. Acad. Sci. U.S.A. 91*, 6948−6952.

23. Imanishi, M., Hori, Y., Nagaoka, M., and Sugiura, Y. (2000) *Biochemistry 39*, 4383−4390.
24. Crothers, D. M., Gartenberg, M. R., and Shrader, T. E. (1991) *Methods Enzymol. 208*, 118−146.
25. Sjøttem, E., Andersen, C., and Johansen, T. (1997) *J. Mol. Biol. 267*, 490−504.
26. Pavletich, N. P., and Pabo, C. O. (1993) *Science 261*, 1701−1707.
27. Clemens, K. R., Liao, X., Wolf, V., Wright, P. E., and Gottesfeld, J. M. (1992) *Proc. Natl. Acad. Sci. U.S.A. 89*, 10822−10826.
28. Nolte, R. T., Conlin, R. M., Harrison, S. C., and Brown, R. S. (1998) *Proc. Natl. Acad. Sci. U.S.A. 95*, 2938−2943.

BI001762+